Towards Reducing Segmentation Labeling Costs for CMR Imaging using Explainable AI

Alessa Stria[a] and Asan Agibetov*[b]

Medical University of Vienna, Center for Medical Statistics, Informatics and Intelligent Systems (CeMSIIS), Institute of Artificial Intelligence, Vienna, Austria

**corresponding author*

Keywords: Deep Learning, Segmentation, Classification, Explainable AI, Class Activation Map, Labeling Costs, Scarce Data, Sample Size Dependence, MRI, Cardiology

Abstract: Provided with a sufficient amount of annotated data, deep learning models have been successfully applied to automatically segment cardiac multi-structures from MR images. However, manual delineation of cardiac anatomical structures is expensive to acquire and requires expert knowledge. Recently, weakly- and self-supervised feature learning techniques have been pro-posed to avoid or substantially reduce the effort of manual annotation. Due to their end-to-end design, many of these techniques are hard to train. In this paper, we propose a simple modular segmentation framework based on U-net architecture that injects class activation maps of separately trained classification models to guide the segmentation process. In a small data setting (20-35% of training data), our framework significantly improved the segmentation accuracy of a baseline U-net model (5%-150%).

1 INTRODUCTION

Segmented cardiac magnetic resonance (CMR) images can computationally quantify significant morphological and pathological changes, such as stroke volume or ejection fraction. These features are essential in cardiac disease quantification and non-invasive pre-clinical diagnosis (Peng et al., 2016). To facilitate the computation of such features, deep-learning-based cardiac segmentation algorithms have been recently proposed in the literature (Bernard et al., 2018; Chen et al., 2020; Oktay et al., 2018). While these algorithms promise the creation of (semi-) automatic segmentation tools, their successful application is heavily conditioned on the availability of large amounts of labeled segmented data. Unfortunately, obtaining segmented MR images is a tedious and time-consuming delineation task that represents a vast challenge in the cardiac imaging domain. While researchers focused on improving the performance, a major challenge in cardiac image segmentation continues to be the scarcity of annotated data (Chen et al., 2020).

Methods focusing on segmentation label dependence reduction include data augmentation (Madani et al., 2018), transfer learning (Tran, 2016), and weakly or self-supervized methods (Oktay et al., 2018; Bai et al., 2019; Ciga and Martel, 2021; Zimmer et al., 2020). These approaches focus on end-to-end framework design, where easily-obtainable classification labels are encoded as an auxiliary prediction task, which, however, can be extremely sensitive to hyperparameter optimization. Instead, we propose a modular design of a segmentation framework decoupled from a classification model in this work.

A classification model can be trained and optimized separately, and its information can be injected into a segmentation model as a separate input channel. Our main hypothesis is that a (pre-trained) AI classification model could be used as a template for segmentation labels. The segmentation framework uses the anatomical priors extracted from a classification model with explainable artificial intelligence (XAI) techniques. Compared to segmentation labels, classification labels, e.g., patient's diagnosis, are much easier to obtain. Indeed, a cardiologist may need to look at a few MR slices and establish the diagnosis, whereas manual segmentation may take hours.

The proposed methodology re-purposes a pre-trained classification model by obtaining the class ac-

[a] https://orcid.org/0000-0003-0178-8867

[b] https://orcid.org/0000-0003-0096-0143

Stria, A. and Agibetov, A.
Towards Reducing Segmentation Labeling Costs for CMR Imaging using Explainable AI.
DOI: 10.5220/0011531200003523
In *Proceedings of the 1st Workshop on Scarce Data in Artificial Intelligence for Healthcare (SDAIH 2022)*, pages 11-16
ISBN: 978-989-758-629-3

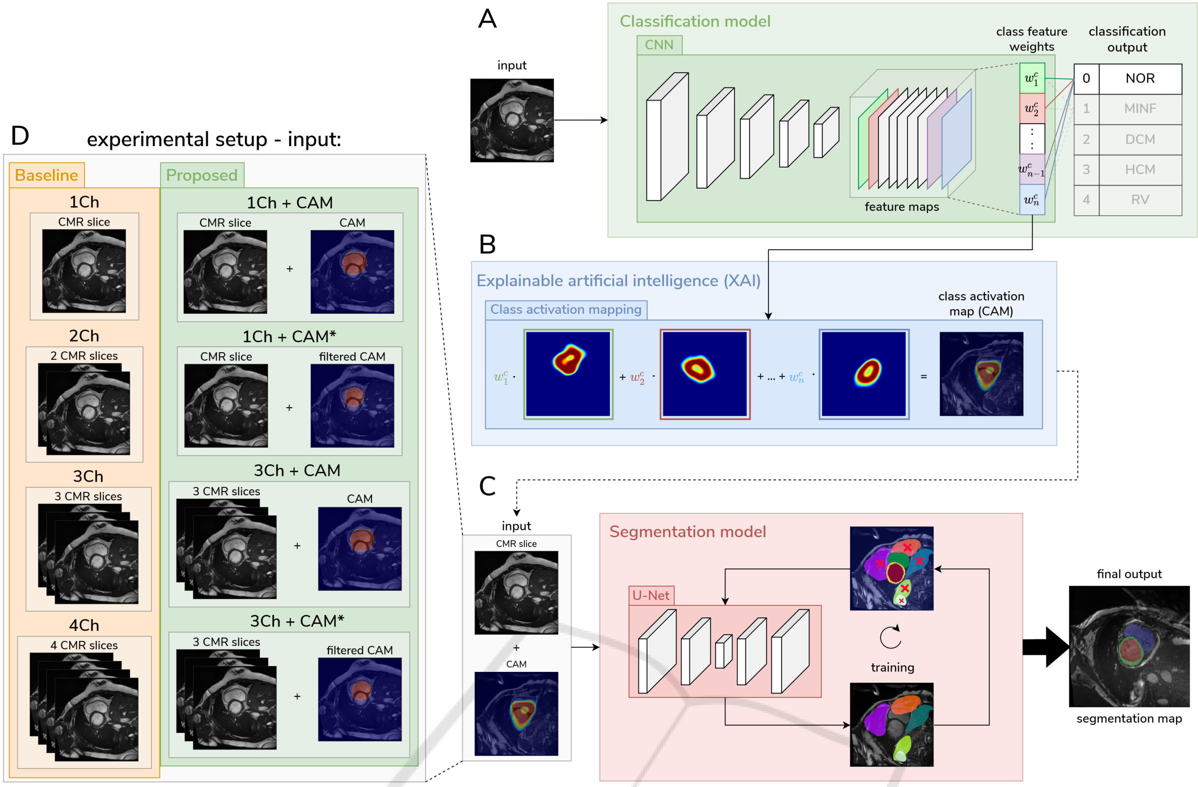

Figure 1: A high-level view of our methodology. Panel A: Training of the classification model. Panel B: Explainable AI technique extract the approximate positions (priors) of the desired anatomical region of interest in the MR image from the classification model. Panel C: These priors are then used as additional input for the segmentation model and reduce the overall search space of possible anatomical regions. Panel D: detailed illustration of the different used input channels for the experiment.

tivation maps (CAMs (Selvaraju et al., 2020)) as segmentation priors. CAM is an explainable AI technique that generates a localization map, which highlights the relevant regions of the image with respect to the prediction of the deep learning model. In this project, Gradient CAMs were used (Selvaraju et al., 2020). These proxy labels are added as an additional input channel to the segmentation model. Therefore, increasing the model complexity and injecting spatial information should constrain the search space. An overview of the methodology is presented in Figure 1.

2 METHODS

2.1 Image Data and Preprocessing

The Automatic Cardiac Diagnosis Challenge (ACDC) dataset from the University Hospital of Dijon, published in 2018, was used for development and evaluation (Bernard et al., 2018). We took cine-MRIs of 100 patients, uniformly distributed over five diagnostic groups (healthy, previous myocardial infarction, dilated cardiomyopathy, hypertrophic cardiomyopathy, abnormal right). Segmentation ground truth masks for all CMRs consists of four classes: background, left ventricle, myocardium, and right ventricle. To prevent information leak-age between training and evaluation, the image data was split into training, validation, and test set (1150, 382, 370 images, respectively).

2.2 Model Specifications

Different convolutional neural network (CNN) architectures were used for the multiclass classification task, including the most common architectures, VGG16 (Simonyan and Zisserman, 2015), Dense-Net (Huang et al., 2017), and ResNet (He et al., 2016). For segmentation models, we used the baseline U-Net architecture (Ronneberger et al., 2015).

Classification models were trained by minimizing categorical cross-entropy loss, where RELU was the used activation function for the convolutional layers. On the final fully-connected layer, the softmax activation function was used. U-net was trained to minimize intersection over union (IoU) metric. VGG16 was optimized with Stochastic gradient descent (SGD), all other classification models with ADAM. For optimization we used learning rate scheduler. On all the models, early stopping was triggered after ten epochs without improvement in the validation loss. To further reduce the risk of overfitting, improve generalization and performance of the classification models, different hyperparameter optimization methods were tested. They include the usage of augmentation on the training set, class weights for the slightly imbalanced classes, different image sizes for more efficient training. We performed a grid search over dropout rates of 0.1, 0.2, and 0.25, number and size of filters in the 11 layered architecture. Different base learning rates included 0.1, 0.01, and 0.001. To reduce the number of filters and the search space, the CMRs were zoomed in to exclude the background.

2.3 Evaluation of Model Performances

Since our interpatient splits were slightly imbalanced, we used the area under the receiver-operating characteristic curve (ROC AUC) as our classification metric. Additionally, we used accuracy and F1 scores. CAMs from our classification network were extracted and primarily compared to the ground truth using the IoU score. In addition, we used Dice similarity coefficient, and Specificity and Sensitivity metrics.

2.4 Sample Size Dependence

The sample size dependency was analyzed by reducing the number of patients in the training and validation set by 5% increments, starting from 100% until 15% sample sizes. The U-Net performance was evaluated by using the mean IoU score. There were different experiments performed to test the impact of input channels and the quality of injected in-formation of our extracted priors: 3 Channel CMR (*3Ch*), 3 Channel CMR + 1 Channel CAM (*3Ch + CAM*), 3 Channel CMR + 1 Channel post-processed CAM (*3Ch + CAM**), 4 Channel CMR (*4Ch*), 1 Channel CMR (*1Ch*), 1 Channel CMR + 1 Channel CAM (*1Ch + CAM*), 1 Channel CMR + 1 Channel post-processed CAM (*1Ch + CAM**), 2 Channel CMR (*2Ch*).

1Ch/2Ch/3Ch/4Ch are baseline models, each representing a single/double/triple/quadruple grayscale image(s). The *3Ch + CAM* and the *1Ch + CAM* represent our proposed methodology. The post-processed CAMs refer to CAMs where a mode filter was applied to smooth the edges of the areas, which is the case for *1Ch + CAM** and *3Ch + CAM**. The mode pixel filter selects the most common pixel value from a box with a specified size — in this case, 12 pixels. Pixel values that occur only once or twice are disregarded. The original pixel value is maintained if there are no pixel values that appear more than twice.

2.5 Experimental Setting

This approach (including data preprocessing, model training, and model evaluation) is developed in Python (version 3.8.12). For deep learning, TensorFlow (version 2.5) was used. All models were trained on the Vienna Scientific Cluster (VSC) with a NVIDIA GTX1080 GPU (8 GB GDDR5) and locally with a NVIDIA GTX 1660 TI (6 GB GDDR5). The medical image segmentation library MISeval (version 1.2) was used for generating CAM tf-keras-vis (version 0.8.1).

3 RESULTS

3.1 The focus of CAM on Important Regions

We trained classification models that look at the whole CMR image as input and predict one of the multiple diagnostic groups. The best performing classification model chosen for the generation of the CAM was a VGG16 architecture that achieved a weighted F1 score of 0.23 and a mean ROC AUC of 0.57. The average IoU score for the CAM of the test set was 0.18, i.e., 18% overlap on all cine MR image slices. When using the post-processed CAM, the IoU was 23%. While the classification performance was low, the IoU in some slices was up to 80%. By visually examining the CAMs of this model, we noticed that it was attending closer to the heart region. The produced segmentation maps from the model were of satisfactory quality, focusing on essential structures (Figure 3). Using different techniques described in the methods section, as well as pre-trained classification models (on ImageNet) yielded no performance gain.

3.2 Extracted Priors from Classification Model Influence Segmentation Performance

Various scenarios of input channels were tested to analyze the influence of injected information on the segmentation performance and what type of content is injected. The best segmentation performance over all different channel combinations Table 1 was obtained

Table 1: Mean IoU segmentation results of all different experiments with varying sample sizes. The values in green represent the best performance for each sample size increment.

percentage	1Ch	1Ch + CAM	1Ch + CAM*	2Ch	3Ch	3Ch + CAM	3Ch + CAM*	4Ch
15	0.250	0.244	0.242	0.241	0.252	0.241	**0.342**	0.245
20	0.242	0.241	0.246	0.241	0.242	0.246	0.305	**0.320**
25	0.241	0.560	0.601	0.309	0.299	0.385	**0.637**	0.316
30	0.343	0.575	0.387	0.254	0.330	**0.649**	0.604	0.298
35	0.616	0.442	0.635	0.613	0.648	**0.695**	0.590	0.661
40	0.483	0.553	0.398	**0.679**	0.604	0.626	0.655	0.665
45	0.434	0.660	0.624	0.648	**0.689**	0.418	0.641	0.369
50	0.475	0.666	0.689	0.654	0.626	**0.697**	0.613	0.397
55	0.675	**0.681**	0.663	0.505	0.678	0.678	0.676	0.468
60	0.617	0.712	0.662	0.639	0.694	0.682	0.685	**0.713**
65	0.364	0.676	0.326	0.242	0.639	0.663	0.684	**0.687**
70	0.692	0.700	**0.741**	0.724	0.703	0.727	0.736	0.661
75	0.663	0.655	0.701	0.715	**0.720**	0.704	0.719	0.715
80	0.684	0.693	0.708	0.686	**0.709**	0.701	0.698	0.707
85	0.572	0.718	0.708	0.730	0.723	**0.735**	0.713	0.679
90	0.684	0.711	0.727	**0.754**	0.737	0.730	0.678	0.730
95	0.730	0.719	0.747	0.689	0.730	0.676	**0.748**	0.727
100	0.721	0.723	0.707	0.732	0.724	0.707	**0.741**	0.681
Average	0.527	0.607	0.584	0.559	0.597	0.609	**0.637**	0.558

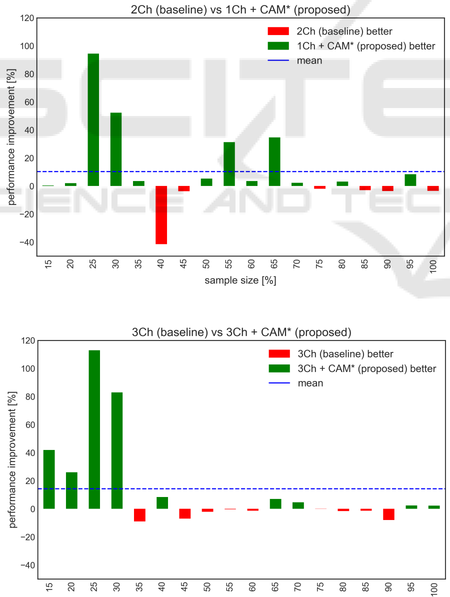

(a)

(b)

Figure 2: Relative performance difference of proposed against the baseline. The x-axes are the percentages, and the y-axis is the relative difference between the models. (a) In the first panel, the *2Ch* is the baseline, and the *1Ch + CAM** is the proposed model. (b) The baseline model *3Ch* is compared against the proposed model *3Ch + CAM**.

with the model using *3Ch + CAM**, with a mean IoU score of 0.637. All Models using the CAM as an additional input channel performs better than the baseline. The highest difference of 0.49 was between the *3Ch + CAM** and the *4Ch*. The lowest performance increase was with *3Ch + CAM* over the *3Ch* with an increase of 0.012 IoU score. Overall, the models with fewer channels (one or two) show a decreased performance compared to those using three or four channels.

Analyzing the relative performance differences (Figure 2), it is apparent that the proposed models significantly outperform the baseline models in the small sample sizes (15-35%). The performance gain is up to 150% improvement in the *1Ch + CAM** case compared to *1Ch* at 25% sample size. In the case of the *3Ch + CAM** against the *3Ch* the improvement at 25% sample size is over 110%.

4 DISCUSSION

In a small data setting (20-35% of training data), our framework significantly improved the segmentation accuracy of a baseline U-net model (5%-150%). These results open a promising research direction that shows that even a far from perfect pre-trained classification model could be used to produce sensible segmentation masks. Our generic methodology might well support the creation of automatic segmentation tools in cardiac MRI that drastically reduce the dependence and thereby the cost of time-consuming delineation labels. The advantage of our approach is its simplicity and robustness to hyperparameter optimization. However, such a decoupled design may prevent a segmentation model of learning features from

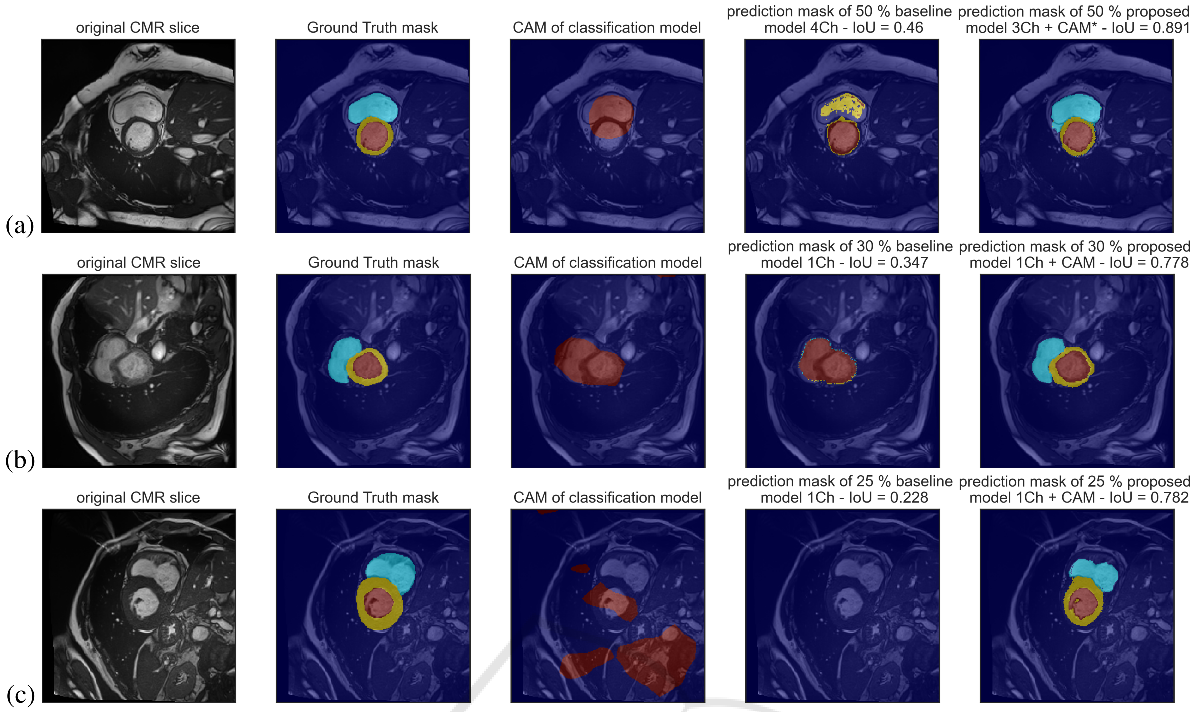
original CMR slice
Ground Truth mask
CAM of classification model
prediction mask of 50 % baseline model 4Ch - IoU = 0.46
prediction mask of 50 % proposed model 3Ch + CAM* - IoU = 0.891
(a)
original CMR slice
Ground Truth mask
CAM of classification model
prediction mask of 30 % baseline model 1Ch - IoU = 0.347
prediction mask of 30 % proposed model 1Ch + CAM - IoU = 0.778
(b)
original CMR slice
Ground Truth mask
CAM of classification model
prediction mask of 25 % baseline model 1Ch - IoU = 0.228
prediction mask of 25 % proposed model 1Ch + CAM - IoU = 0.782
(c)

Figure 3: Example outputs of predictions masks from a baseline model and a proposed model with the CMR slice in the background for different scenarios. Panel (a), prediction from models with 50% sample size, baseline model is *4ch*, prediction model is *3Ch + CAM**. Panel (b), prediction from models with 30% sample size, baseline model is *1ch*, prediction model is *1Ch + CAM*. The CAM represents the heart region and is comparable to the baseline prediction. The baseline predicts only two classes, the IoU score is low, the prediction model outperforms the baseline model. Panel (c), prediction from models with 25% sample size, baseline model is *1ch*, prediction model is *1Ch + CAM*. The CAM is dispersed without focusing on the heart region. The proposed model outperforms the baseline model, it only predicts the background class and thereby only achieves an IoU of 0.228. However, with the additional injected information of the CAM, the proposed model achieves an IoU of 0.782.

auxiliary classification tasks. A thorough comparison of our approach to end-to-end multi-task methods is part of our future work.

The segmentation performance increases in most cases if the model complexity is increased. Therefore, using additional channels and increasing the number of variables in the model improves the performance. However, it matters which performance is used in the additional channels. The baseline models - with the same amount of channels as the models where CAMs are used as an additional input are *2Ch* and *4Ch* – have a decreased performance as our proposed models. Injecting CAMs improve the segmentation performance since they constrain the search space with the spacial information given from the priors.

As this is a work in progress we are fully aware of the current limitations of our approach. Using the proposed methodology on a dataset with higher classification performance could improve segmentation performance. Due to the computational complexity, we have not properly quantified the uncertainty of all models, and we only performed a shallow hyperparameter optimization. Finally, the CMRs were used as single 2D images, which do not represent the 3D structure of the heart, and spatial information is lost. Additionally, the heart regions in the end and beginning slices of each cardiac phase are almost nonexisting, and thereby a segmentation model trained only with the 2D input will perform poorly at these slices. Future work should address these limitations and analyze the per-class performance gain.

FUNDING

This research was funded by ÖKG Forschungsstipendium ”Reducing costs of segmentation labeling in cardiac MRI using explainable AI”.

ACKNOWLEDGEMENTS

The computational results were partly achieved by using the Vienna Scientific Cluster (VSC)

CONFLICTS OF INTEREST

The authors declare no conflict of interest.

REFERENCES

Bai, W., Chen, C., Tarroni, G., Duan, J., Guitton, F., Petersen, S. E., Guo, Y., Matthews, P. M., and Rueckert, D. (2019). Self-Supervised Learning for Cardiac MR Image Segmentation by Anatomical Position Prediction. In Shen, D., Liu, T., Peters, T. M., Staib, L. H., Essert, C., Zhou, S., Yap, P.-T., and Khan, A., editors, *Medical Image Computing and Computer Assisted Intervention – MICCAI 2019*, volume 11765, pages 541–549. Springer International Publishing, Cham.

Bernard, O., Lalande, A., Zotti, C., Cervenansky, F., Yang, X., Heng, P.-A., Cetin, I., Lekadir, K., Camara, O., Gonzalez Ballester, M. A., Sanroma, G., Napel, S., Petersen, S., Tziritas, G., Grinias, E., Khened, M., Kollerathu, V. A., Krishnamurthi, G., Rohe, M.-M., Pennec, X., Sermesant, M., Isensee, F., Jager, P., Maier-Hein, K. H., Full, P. M., Wolf, I., Engelhardt, S., Baumgartner, C. F., Koch, L. M., Wolterink, J. M., Isgum, I., Jang, Y., Hong, Y., Patravali, J., Jain, S., Humbert, O., and Jodoin, P.-M. (2018). Deep Learning Techniques for Automatic MRI Cardiac Multi-Structures Segmentation and Diagnosis: Is the Problem Solved? *IEEE Transactions on Medical Imaging*, 37(11):2514–2525.

Chen, C., Qin, C., Qiu, H., Tarroni, G., Duan, J., Bai, W., and Rueckert, D. (2020). Deep Learning for Cardiac Image Segmentation: A Review. *Frontiers in Cardiovascular Medicine*, 7:25.

Ciga, O. and Martel, A. L. (2021). Learning to segment images with classification labels. *Medical Image Analysis*, 68:101912.

He, K., Zhang, X., Ren, S., and Sun, J. (2016). Identity mappings in deep residual networks. In Leibe, B., Matas, J., Sebe, N., and Welling, M., editors, *Computer Vision – ECCV 2016*, pages 630–645, Cham. Springer International Publishing.

Huang, G., Liu, Z., Van Der Maaten, L., and Weinberger, K. Q. (2017). Densely connected convolutional networks. In *2017 IEEE Conference on Computer Vision and Pattern Recognition (CVPR)*, pages 2261–2269.

Madani, A., Ong, J. R., Tibrewal, A., and Mofrad, M. R. K. (2018). Deep echocardiography: Data-efficient supervised and semi-supervised deep learning towards automated diagnosis of cardiac disease. *npj Digital Medicine*, 1(1):1–11.

Oktay, O., Ferrante, E., Kamnitsas, K., Heinrich, M., Bai, W., Caballero, J., Cook, S. A., de Marvao, A., Dawes, T., O'Regan, D. P., Kainz, B., Glocker, B., and Rueckert, D. (2018). Anatomically Constrained Neural Networks (ACNNs): Application to Cardiac Image Enhancement and Segmentation. *IEEE Transactions on Medical Imaging*, 37(2):384–395.

Peng, P., Lekadir, K., Gooya, A., Shao, L., Petersen, S. E., and Frangi, A. F. (2016). A review of heart chamber segmentation for structural and functional analysis using cardiac magnetic resonance imaging. *Magnetic Resonance Materials in Physics, Biology and Medicine*, 29(2):155–195.

Ronneberger, O., Fischer, P., and Brox, T. (2015). U-net: Convolutional networks for biomedical image segmentation. In Navab, N., Hornegger, J., Wells, W. M., and Frangi, A. F., editors, *Medical Image Computing and Computer-Assisted Intervention – MICCAI 2015*, pages 234–241, Cham. Springer International Publishing.

Selvaraju, R. R., Cogswell, M., Das, A., Vedantam, R., Parikh, D., and Batra, D. (2020). Grad-CAM: Visual Explanations from Deep Networks via Gradient-Based Localization. *International Journal of Computer Vision*, 128(2):336–359.

Simonyan, K. and Zisserman, A. (2015). Very deep convolutional networks for large-scale image recognition. In *International Conference on Learning Representations*.

Tran, P. V. (2016). A fully convolutional neural network for cardiac segmentation in short-axis mri. *ArXiv*, abs/1604.00494.

Zimmer, V. A., Gomez, A., Skelton, E., Ghavami, N., Wright, R., Li, L., Matthew, J., Hajnal, J. V., and Schnabel, J. A. (2020). A Multi-task Approach Using Positional Information for Ultrasound Placenta Segmentation. In Hu, Y., Licandro, R., Noble, J. A., Hutter, J., Aylward, S., Melbourne, A., Abaci Turk, E., and Torrents Barrena, J., editors, *Medical Ultrasound, and Preterm, Perinatal and Paediatric Image Analysis*, volume 12437, pages 264–273. Springer International Publishing, Cham.